

The recognition and modelling of a backbone and its deformity

Ramūnas Markauskas^a, Algimantas Juozapavičius^a, Kęstutis Saniukas^b,
Giedrius Bernotavičius^b

^aFaculty of Mathematics and Informatics, Vilnius University
Naugarduko str. 24, LT-03225 Vilnius, Lithuania
ramunas.markauskas@mif.vu.lt; algimantas.juozapavicius@mif.vu.lt

^bVilnius University Hospital Santariškių Klinikos
Santariškių str. 2, LT-08406 Vilnius, Lithuania
saniukas@gmail.com; g.bernotavicius@gmail.com

Received: 25 February 2013 / **Revised:** 18 August 2013 / **Published online:** 25 November 2013

Abstract. In this article the authors present a method for the backbone recognition and modelling. The process of recognition combines some classical techniques (Hough transformation, GVF snakes) with some new (authors present a method for initial curvature detection, which they call the Falling Ball method). The result enables us to identify high-quality features of the spine and to detect the major deformities of backbone: the intercrestal line, centre sacral vertical line, C7 plumbline; as well as angles: proximal thoracic curve, main thoracic curve, thoracolumbar/lumbar. These features are used for measure in adolescent idiopathic scoliosis, especially in the case of treatment. Input data are just radiographic images, meet in everyday practice.

Keywords: active contours, Hough, Falling Ball, mathematical modelling of the backbone, adolescent idiopathic scoliosis, spinal deformities, recognition.

1 Introduction

Rapid technological advancement contributes to the increasing use of digital radiographs in the clinical routine. It offers a diverse application of digital processing techniques to find suitable patterns in x-ray images, to improve the quality of these images, and to organise a fast and efficient storage of them in databases [1]. Another positive aspect of digital technology is the use of a systematic assessment method which may reduce the impact of errors related to human subjectivity [2, 3].

Adolescent idiopathic scoliosis (AIS) is the most common type of abnormal (deformity) curvature of a spine. In over 80% of the cases, it is diagnosed and rapidly progresses during the human growth period [4]. A normal human spine has a physiological sagittal curvature where the upper curvature shows kyphosis in the thoracic region and the lower curvature denotes lordosis in the lumbar spinal region [5].

Idiopathic scoliosis is defined as curvature of the spine in frontal plane of at least 10°, with the rotation of the vertebral bodies, of unknown origin [6,7]. The risk of the curvature progression increases in the fastest growth period of a patient's body, in particular, during puberty.

Scoliosis with a significant curvature in the patient's frontal plane requires immediate treatment (most probably surgical), as it is very likely to lead to disability and changes in posture. The conventional clinical method to diagnose a spinal deformity is based on therapists' subjective assessment, by measuring typical angles of the scoliosis curve directly from the posterior/anterior (PA) and lateral x-ray images [8,9], or by the image processing technique such as a newly introduced low dose ionising system [7].

Visualising and understanding spinal deformities, including idiopathic scoliosis, needs to be quantified and described in a reliable manner. Quantifying the deformity facilitates developing a clear understanding of the important structural features of the altered spinal anatomy, necessary to develop an effective treatment plan. Equally important, it facilitates accurate communication among healthcare providers, allowing them to carry out a comparative analysis of alternative treatment regimens for similar deformities. The most important features of the description of a quantitative spinal deformity are as follows:

- intercrestal line (ICL) which confirms the location and direction of vertebra L5 in a typical case, and L6 or L4 in an atypical case, in the coronal plane;
- centre sacral vertical line (CSVL) which is drawn from the middle of S1 upwards and parallels the vertical edge of a radiograph;
- regional curves, including proximal thoracic (PT) curve, main thoracic (MT) curve and thoracolumbar/lumbar (TL/L) curve, as the main tool of the coronal Cobb measurement;
- C7 plumb line (C7PL) which is dropped down from the middle of the C7 vertebral body, parallel to the vertical edge of a radiograph;
- tilt angle and clavicle angle. A tilt angle is drawn between the zenith line of the first ribs and the line perpendicular to the vertical edge of a radiograph, while a clavicle angle is drawn between a horizontal reference line and a line which touches the most cephalad aspect of both the right and the left clavicle.

Recently, there were some attempts to measure spinal deformity quantitatively, in an automatic way. Most notable is mentioned in [10], where the images were examined to evaluate Cobb angle variability, end plate selection, as well as intra- and inter-observer errors. The objective of this study is to assess the reliability of computer-assisted Cobb angle measurements taken from digital x-ray images. Another article is in [11]. This article reviews the options that currently exist for image guidance in spine surgery and the literature on clinical applications of image-guided techniques in spine surgery.

This paper presents a new approach to the process of segmentation and bone recognition, as well as to the computation of parameters of a quantitative spinal deformity. This approach not only has segmented the spine and recognises it as an image, but also prescribes a theoretical mathematical curve to it. This gives a suitable abstraction of the environment of the spine and allows us to calculate many features for the support

system of a human body, such as the Cobb angle, CSVL, C7PL, proximal thoracic, main thoracic, thoracolumbar curves, pedicles, etc., that are so valuable in computer-assisted spinal surgeries.

2 The theoretical model of spine

The principal scheme of the algorithm for a mathematical spinal curvature is illustrated in Fig. 1. Once the excessive data are removed from the original image by different methods, the aim is to locate the clavicle and the pelvis. These objects define the top and bottom edges of the spine. The approximate position of the spinal curvature, which is approximated by a spline and expanded to embrace the contour of the spine, is detected by the so-called Falling Ball method. The contour of the spine is revised with a help of the active contours method, and the resultant contour is approximated by a spline. The paper further describes the algorithm step by step.

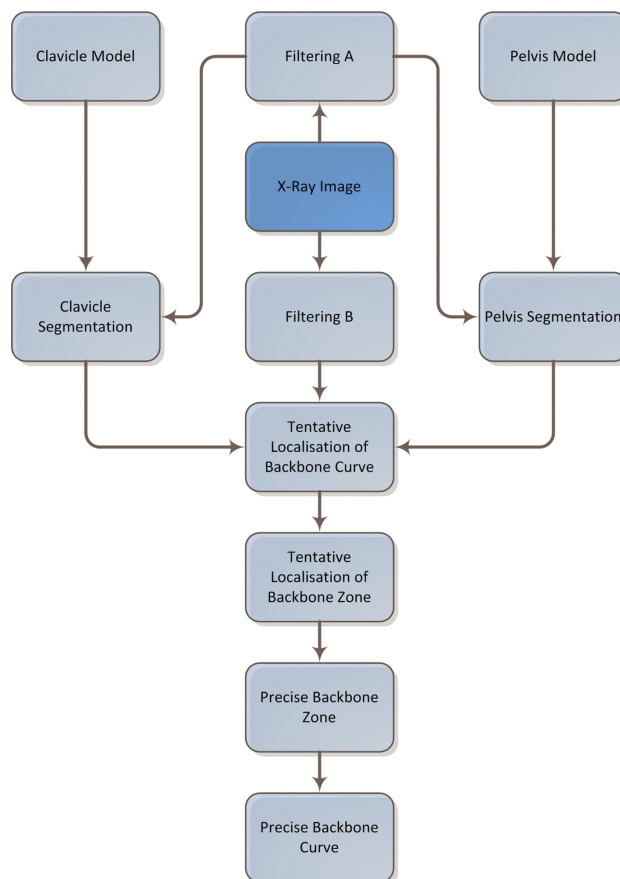


Fig. 1. Principal scheme of the algorithm.

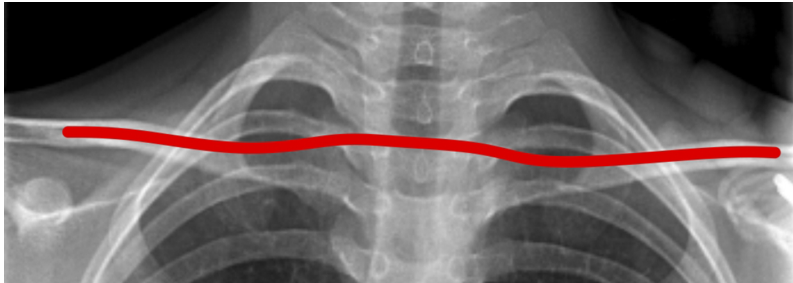


Fig. 2. Model of the clavicle.

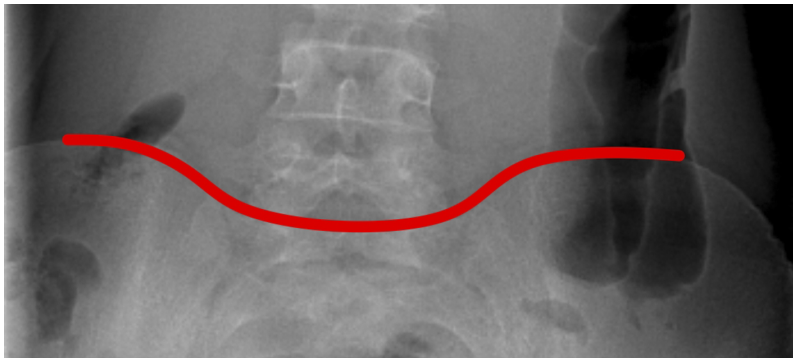


Fig. 3. Model of the pelvis.

2.1 Model of the clavicle

A model of the clavicle (Fig. 2) is build manually by repeating all contours that are visible in a real x-ray image. The resultant contour (formed by the clavicle (clavicula) and the thoracic vertebrae (vertebra thoracica) is expressed in a binary matrix $N \times M$, but will be replaced in further studies by a polynomial function.

2.2 Model of the pelvis

A model of the pelvis (Fig. 3) is build manually by repeating all contours that are visible in a real x-ray image. The resultant contour (formed by iliac crests (crista iliaca) and the upper part of the sacrum (os sacrum) is expressed in a binary matrix $N \times M$, but will be replaced in further studies by a polynomial function.

2.3 Filtering A

This type of filtering prepares an x-ray for detecting a model of the clavicle and the pelvis. The method as such may be broken down into brightness equalisation, blurring, filtering and conversion into a binary image (Fig. 4). An example of a filtered image is provided in Fig. 5.

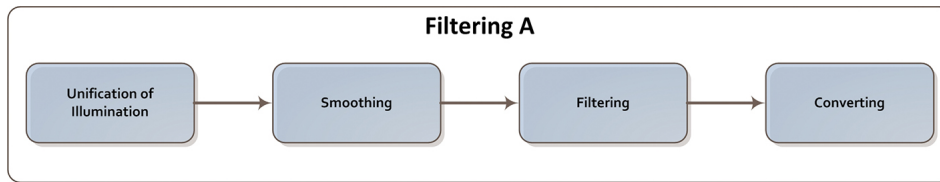


Fig. 4. Steps of Filter A.

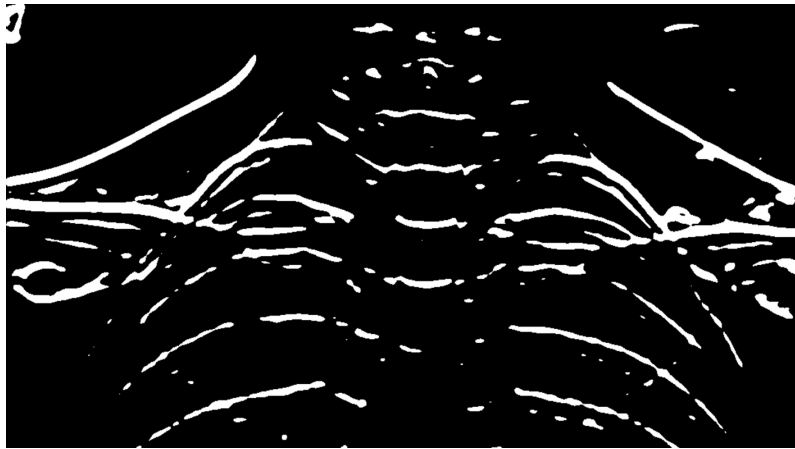


Fig. 5. Results of filtering A of the clavicle area.

2.3.1. Brightness equalisation. This process is based on [12]. It adjusts the linear plane to the intensity of the image. The linear plane is then removed from the original image, thus eliminating shadow/non-unified illumination effects.

2.3.2. Blurring. At this stage, the Gaussian convolution filter with a kernel of 50×50 and $\sigma = 4$, calculated in accordance with formula (1) is used for smoothing the image [13].

$$G(x, y, \sigma) = \frac{1}{2\pi\sigma^2} e^{-(x^2+y^2)/(2\sigma^2)} \quad (1)$$

2.3.3. Filtering. The convolution filter with a kernel rendered in (2) highlights horizontal objects which are marks of the clavicle and the pelvis.

$$\begin{bmatrix} -1 & -2 & -3 & -2 & -1 \\ 0 & 0 & 0 & 0 & 0 \\ 1 & 2 & 3 & 2 & 1 \end{bmatrix} \quad (2)$$

2.3.4. Conversion. The results obtained are converted into a binary image, where the clavicle is subject to the limit of 2.5% and the pelvis to the limit of 1%.

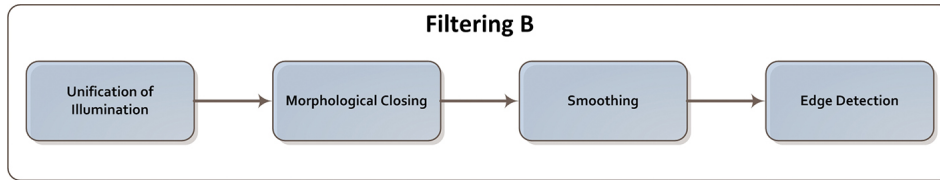


Fig. 6. Steps of filtering B.

2.4 Filtering B

This type of filtering prepares an x-ray image for detecting contours and the curvature of the spine. The method as such may be broken down into brightness equalisation, morphological closing, blurring, and edge detection (Fig. 6).

2.4.1. Brightness equalisation. The method of brightness equalisation is identical to the one used in filtering A.

2.4.2. Morphological closing. The closing includes image erosion and dilatation procedures (for more see [13]), with a disc-shaped structuring element with radius $20\ 39 \times 39$. These procedures combine individual elements of an image, thereby forming a one-piece contour of the spine.

2.4.3. Blurring. The blurring process is identical to the one used in filtering A, only with different parameters: a kernel of 10×10 and $\sigma = 5$.

2.4.4. Edge detection. Edges are located with the help of the Canny edge detection algorithm (for more see [14–16]).

2.5 Location of the clavicle

Model fitting is used to find the position of the clavicle in an x-ray image. Fig. 7 illustrates how the model fits (the number of matching points) in terms of points in the original image.

2.6 Location of the pelvis

Model fitting is used to find the position of the pelvis in an x-ray image. Fig. 8 illustrates how the model fits (the number of matching points) in terms of points in the original image.

2.7 Finding the preliminary curve of the spine

The authors suggest establishing the preliminary position of the spine with the Falling Ball method (the mathematical expression is presented in formula

$$P_i = P_{i-1} + S(P_i) + S_b + S(P_{i-1}) \times k. \quad (3)$$

Here P_i – position of the ball at moment i , $S(P_i)$ – gradient vector flow that effects position i , S_b – basic force field, k – resistance ration. This method is based on the

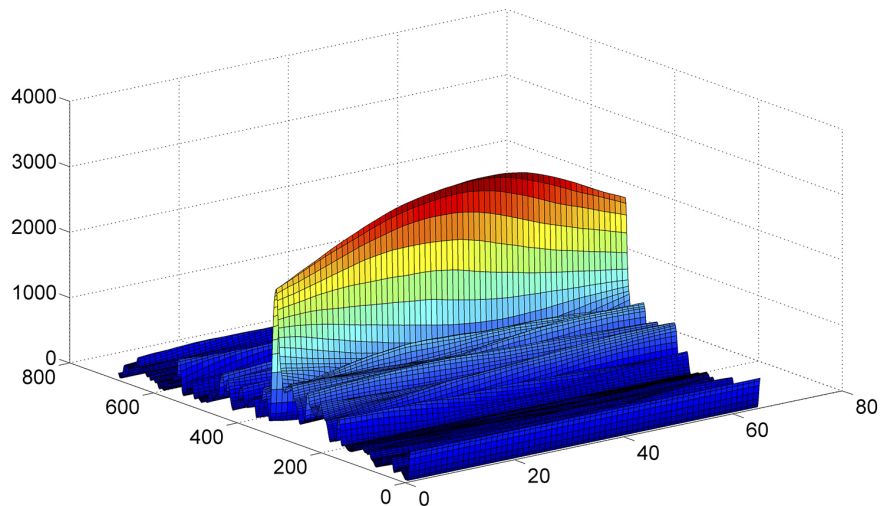


Fig. 7. Clavicle model fitting.

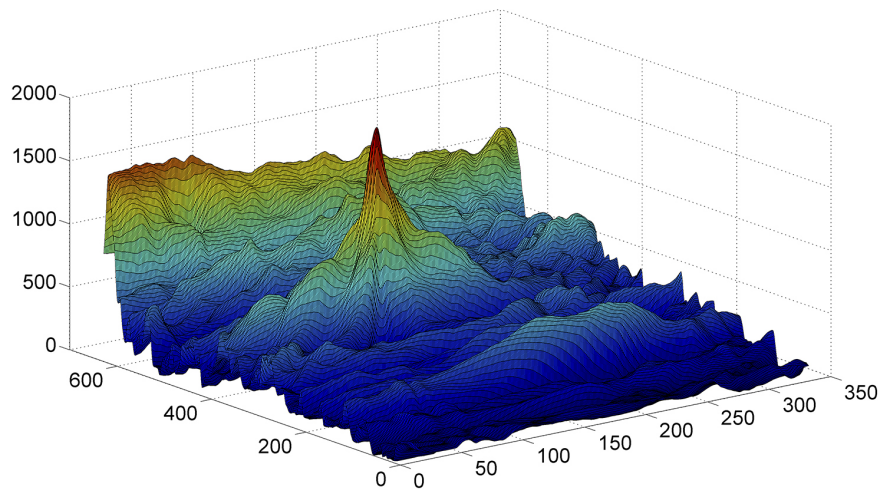


Fig. 8. Pelvis model fitting.

ordinary perception of the environment. Imagine that the spine is a tube and you send a ball down this tube. The ball is falling down affected by the gravitation, changing its directions due to the obstacles (i.e. walls of the spine) encountered on its way down. The trajectory of the falling ball is recorded and its points become the initial approximate position of the spine. The starting point of the trajectory is the detected position of the clavicle, and the end point – the detected position of the pelvis.

For the results of the method, see Fig. 9.

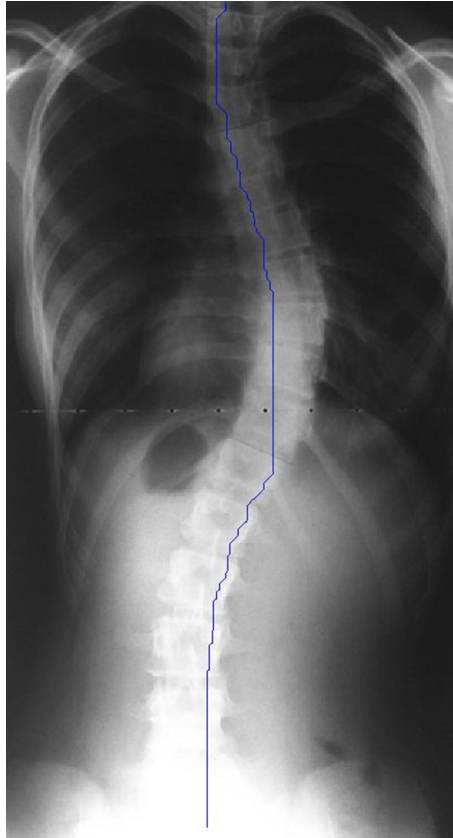


Fig. 9. Preliminary curve of the spine.

2.8 Preliminary region of the spine

The preliminary region of the spine is found with a help of the preliminary position of the spine: it is expanded by the horizontal axis at equal distances in both directions, and the resultant new curves are connected (Fig. 10).

2.9 Revised region of the spine

The region of the spine is revised on the basis of the active contour algorithm provided by Xu and Prince [17]. The algorithm address key problems faced by other acting contour algorithms, namely, the progressing contour towards distant objects and regular bypass of concave objects. The authors call their method the Gradient Vector Flow (GVF) snake [18]. The first step in this algorithm is the calculation of force fields in the image (in our case – in an x-ray image). This field is a driving force for bending, stretching and deforming a snake to converge contours of the object detected. It can be found by applying

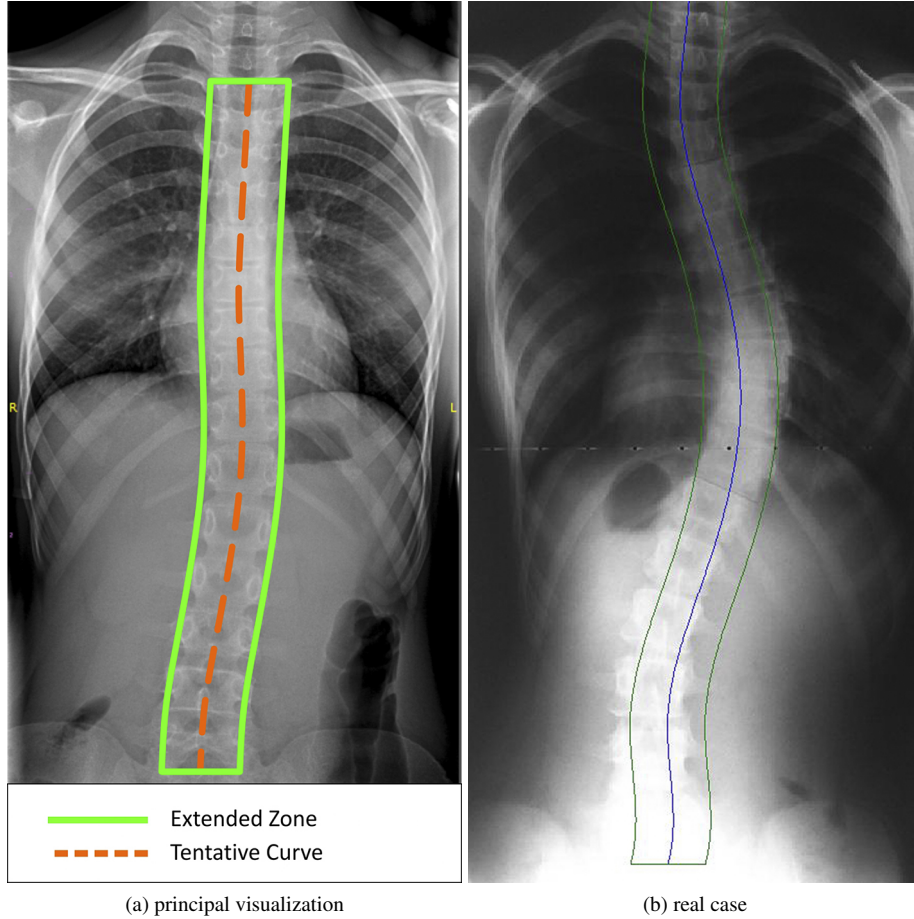


Fig. 10. Preliminary curve and region of the spine.

generalised diffusion equations to a horizontal as well as vertical image gradient, solving Euler equations

$$\begin{aligned} \mu \nabla^2 u - (u - f_x)(f_x^2 + f_y^2) &= 0, \\ \mu \nabla^2 v - (v - f_x)(f_x^2 + f_y^2) &= 0, \end{aligned} \tag{4}$$

where ∇^2 is the Laplacian operator [19]. Diffusion forms a force field further from the object, thus allowing the snake to reach remote and concave objects. A GVF snake is a parametric curve by which the dynamic equation

$$x_t(s, t) = \alpha x''(s, t) - \beta x'''(s, t) + v, \tag{5}$$

where v is a calculated vector field [17], is solved. All the steps above are focused on preparing an x-ray for this algorithm and establishing the main parameters, i.e. the initial

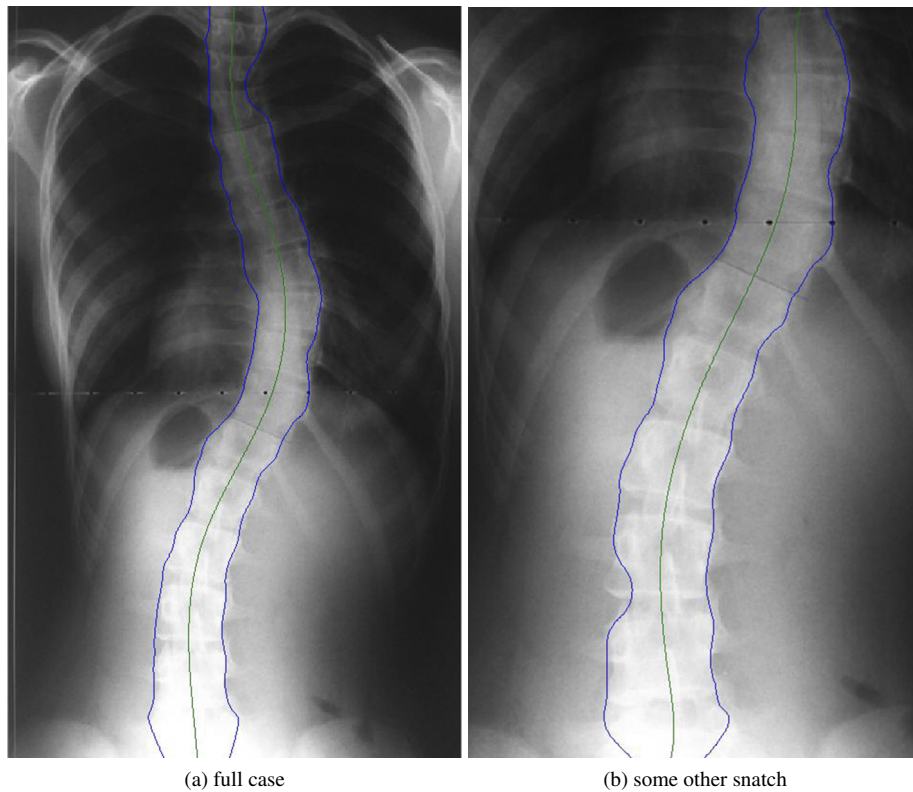


Fig. 11. Final results.

detection region. The detection itself takes place in the MatLab environment, using the code [20] provided by the authors of the algorithm.

2.10 Curvature of the spine

The resultant contour of the GVF snake is approximated by the spline, using 6 breaking points [21]. The results are presented in Fig. 11.

3 The application of a spine model

The spine has characteristic alignment in the coronal plane, where it is (or has to be) straight. It is clear that understanding normal and abnormal spinal anatomy and our ability to clearly describe it is important. A description of spinal deformities like whole methodology in medical-geometry terms is presented in [22]. Model presented in this article can be further extended to extract features used in classification/diagnosis of spinal deformity by following means:

- *Pelvic Coronal Reference Line (PCRL), Intercrestal Line (ICL) extraction*: pelvis model, which is defined as contour formed by iliac crests (crista iliaca) and the upper part of the sacrum (os sacrum), is fitted to the x-ray and PCRL or ICL line is defined as one passing through the top of iliac crests (crista iliaca) – calculations can be applied to extract this line from the pelvis model.
- *Central Sacral Vertical Line (CSVL) extraction*: the upper part of the sacrum which is extracted by pelvis model is perpendicular to CSVL.
- *Clavicle Reference Line (CRL) extraction*: clavicle model, which is defined as contour formed by both left and right clavicles (clavicula) and the thoracic vertebrae (vertebra thoracica), is fitted to the x-ray and CRL line is defined as one passing through the top of clavicles (clavicula) – calculations can be applied to extract this line from clavicle model.
- *Coronal Cobb Measurements (Proximal Thoracic (PT), Main Thoracic (MT) and Thoracolumbar/Lumbar (TL/L) Curves)*: spinal curve in the final result is defined as spline with 6 knots. The amount of knots can be fined tuned to fit the principal of Cobb measurements (curves are measured from vertebrae which indicates change of the spine curvature) and the idea of spline (knots are points where polynomial pieces of the spline connect). That will give an opportunity to identify points from where calculations should be made to get the right curves one seek.

The future research is intended to cover a few topics. One is to assessing spinal deformity as subjective by evaluating the characteristic angles and other properties of spinal curve from a set of radiographic images. The other, most interesting case are parameterized 3D anatomical models of the spine, to quantitatively assess the deformity, different ways of stretch, as well as to minimize the amount of radiation exposure by reducing the number of radiographs required. The main components of this modelling system will be a 3D parametric solid model of spine, back surfaces, relevant clinical information and scoliosis ontology.

References

1. M. Gstoettner, K. Sekyra, N. Walochnik, P. Winter, R. Wachter, C.M. Bach, Inter- and intraobserver reliability assessment of the cobb angle: Manual versus digital measurement tools, *Eur. Spine J.*, **16**(10):1587–1592, 2007.
2. S. Champain, K. Benchikh, A. Nogier, C. Mazel, J.D. Guise, W. Skalli, Validation of new clinical quantitative analysis software applicable in spine orthopaedic studies, *Eur. Spine J.*, **15**(6):982–991, 2006.
3. S. Allen, E. Parent, M. Khorasani, D.L. Hill, E. Lou, J.V. Raso, Validity and reliability of active shape models for the estimation of cobb angle in patients with adolescent idiopathic scoliosis, *J. Digit. Imaging*, **21**(2):208–218, 2008.
4. J. Boisvert, F. Cheriet, X. Pennec, H. Labelle, N. Ayache, Articulated spine models for 3-D reconstruction from partial radiographic data, *IEEE Trans. Biomed. Eng.*, **55**(11):2565–2574, 2008.

5. S. Benameur, M. Mignotte, S. Parent, H. Labelle, W. Skalli, J. de Guise, 3D/2D registration and segmentation of scoliotic vertebrae using statistical models, *Comput. Med. Imag. Grap.*, **27**(5):321–338, 2003.
6. N. Boos, M. Aebi, *Spinal Disorders: Fundamentals of Diagnosis and Treatment*, Springer, 2008.
7. H. Labelle, C. Aubin, R. Jackson, L. Lenke, P. Newton, S. Parent, Seeing the spine in 3D: How will it change what we do?, *J. Pediatr. Orthop.*, **31**(1 Suppl.):37–45, 2011.
8. H. Li, W. Leow, C. Huang, T. Howe, *Modeling and Measurement of 3D Deformation of Scoliotic Spine Using 2D X-Ray Images*, Springer, 2009, pp. 647–654.
9. H. Lin, Identification of spinal deformity classification with total curvature analysis and artificial neural network, *IEEE Trans. Biomed. Eng.*, **55**(1):376–382, 2008.
10. M.C. Tanure, A.P. Pinheiro, A.S. Oliveira, Reliability assessment of cobb angle measurements using manual and digital methods, *The Spine Journal*, **10**(9):769–774, 2010.
11. A.A. Patel, P.G. Whang, A.R. Vaccaro, *Overview of Computer-Assisted Image-Guided Surgery of the Spine*, Elsevier, 2008, pp. 186–194.
12. Amro, How to improve image quality in Matlab, <http://stackoverflow.com/questions/6575366/how-to-improve-image-quality-in-matlab>, 2011.
13. J. Russ, *The Image Processing Handbook*, 6th edition, Taylor & Francis, 2011.
14. J. Canny, A computational approach to edge detection, *IEEE Trans. Pattern Anal. Mach. Intell.*, **6**:679–698, 1986.
15. L. Ding, A. Goshtasby, On the canny edge detector, *Pattern Recognition*, **34**(3):721–725, 2001.
16. R. Wang, Canny edge detection, <http://fourier.eng.hmc.edu/e161/lectures/canny/node1.html>, 2008.
17. C. Xu, J. Prince, Gradient vector flow: A new external force for snakes, in: *Proceedings of the 1997 Conference on Computer Vision and Pattern Recognition (CVPR'97)*, IEEE, 1997, pp. 66–71.
18. C. Xu, J.L. Prince, Active contours, deformable models, and gradient vector flow, <http://www.iacl.ece.jhu.edu/static/gvf/>, 1998.
19. C. Xu, J. Prince, Snakes, shapes, and gradient vector flow, *IEEE Trans. Image Process.*, **7**(3):359–369, 1998.
20. C. Xu, J.L. Prince, GVF, http://www.nitrc.org/frs/download.php/1962/gvf_v5.zip, 1999.
21. J. Lundgren, SPLINEFIT, <http://www.mathworks.com/matlabcentral/fileexchange/13812-splinefit>, 2011.
22. M.F. O'Brien, T.R. Kuklo, K.M. Blanke, L.G. Lenke (Eds.), *Radiographic Measurement Manual*, The Spinal Deformity Study Group, Medtronic Sofamor Danek, USA, 2008.